*Nucleic Acids Research, 2006, Vol. 34, No. 10* ***e75***
*doi:10.1093/nar/gkl364*

# Electrochemical detection of mismatched DNA using a MutS probe

**Minseon Cho, Sohyun Lee, Se-Young Han, Jin-Young Park, Md Aminur Rahman[1], Yoon-Bo Shim[1,*] and Changill Ban***

Department of Chemistry, Pohang University of Science and Technology, Pohang, Gyungbuk, 790-784, South Korea and [1]Department of Chemistry, Pusan National University, Busan, 609-735, South Korea

Received November 12, 2005; Revised November 20, 2005; Accepted April 25, 2006

## ABSTRACT

**A direct and label-free electrochemical biosensor for the detection of the protein–mismatched DNA interaction was designed using immobilized N-terminal histidine tagged *Escherichia coli.* MutS on a Ni-NTA coated Au electrode. General electrochemical methods, cyclic voltammetry (CV), electrochemical quartz crystal microbalance (EQCM) and impedance spectroscopy, were used to ascertain the binding affinity of mismatched DNAs to the MutS probe. The direct results of CV and impedance clearly reveal that the interaction of MutS with the CC heteroduplex was much stronger than that with AT homoduplex, which was not differentiated in previous results (GT > CT > CC ≈ AT) of a gel mobility shift assay. The EQCM technique was also able to quantitatively analyze MutS affinity to heteroduplexes.**

## INTRODUCTION

Various interactions between biomolecules reveal many of the phenomena appearing *in vivo*. Knowledge of the diverse role of biomolecules *in vivo* assists in the discovery of disease inducing factors, the development of new medicines and applications for biochips/biosensors. In particular, DNA–protein interactions have been investigated intensively for decades since they have crucial roles in cellular mechanisms such as transcriptional regulation (1) or mismatch DNA repair systems (2). The detection of a protein–DNA interaction has been advanced through traditional protracted methods, such as the gel-shift assay (3,4), filter binding assay (5) and the DNA footprint assay (6). The creation of a new and expedient method to detect the specific DNA-binding activity of a protein is desirable due to its wide applicability in rapidly developing biological research.

Recently several detection methods for protein–DNA interactions have been developed with optical, electrochemical, surface acoustics spectroscopic and micro gravimetric techniques. Of these methods, the electrochemical methods offer a sensitive, selective, low cost and miniaturized device for the detection of biological molecules (7–12). Electrochemical transducers monitor the signals of current, potential, conductivity and impedance during the interaction between the probe and the target. Of various electrochemical methods, CV is an important analytical technique for the diagnosis of electron transfer reaction in the field of chemistry and biology. In CV, the current flow in the cell is measured as a function of potential. The potential of an electrode in a solution is linearly cycled from a starting potential to a final potential and reversed to the starting potential. CV traces the transfer of electrons during an oxidation–reduction (redox) reaction. The transfer of electrons create current, the magnitude of which can give us clues about our substances. On the other hand, the impedance spectroscopy involves the application of a sinusoidal electrochemical perturbation (potential or current) to the sample that covers a wide range of frequencies. Impedance analysis allows the detection of capacitance, reactance and resistance changes at the interfaces that originate from surface species. The capacitance and resistance changes upon the surface species formation at the electrode surface can be derived from the imaginary part ($Z_{im}$) and real part ($Z_{real}$), respectively, of the Nyquist plot of impedance spectrum. The impedance spectroscopy is also used to monitor the variation of impedance value (in Bode plot) before and after the interaction of the probe with analytes. The impedance changes reflect the degree of interaction between the probe and the target. Thus, voltammetric and impedance methods can measure the interaction between biomolecules appearing at the surface of an electrode. By construction of appropriate compounds for attaching biomolecules onto the electrode surface or by the preparation of chemical functional groups in biomolecules for direct attachment to the electrode surface, detection of DNA–protein interaction (13), DNA hybridization (10,14–17) and antigen–antibody interaction (18) are all facilitated. When these interactions appear, changes in impedance of the electrode surface and hence in the electric current signal allow

*To whom correspondence should be addressed. Tel: +82 54 279 2127; Fax: +82 54 279 3399; Email: ciban@postech.ac.kr
*Correspondence may also be addressed to Yoon-Bo Shim. Tel: +82 51 510 2244; Fax: +82 51 516 7421; Email: ybshim@pusan.ac.kr

quantitative measurement of the extent of the interaction, from which the roles and functions of the molecules may be inferred (19,20).

Since MutS and its homologs in many organisms can specifically recognize and bind all possible base–base mismatches and insertions/deletions (21–23), they can be used to detect mismatched DNA in the electrochemical method (24,25), surface plasmon resonance (SPR) (26,27) and the electrochemical quartz crystal microbalance (EQCM) (28) as well as other biochemical methods (3–6). For the immobilization of DNA probe on a gold surface, DNA sequences with a thiol group (25) or a biotin–streptavidin–biotin bridge (28) have been used in recent years. However, these methods were limited to be used as disposable sensors. In addition, SPR, an expensive device, has difficulty detecting low concentration or low molecular mass analytes. Thus, it needs to develop a robust method for the detection of the proteins–DNA interaction. To do this, MutS protein was examined, because it has the unique property to repair mismatches of DNA.

Several studies have shown that MutS has variable affinities for different mismatches (29–32). MutS forms the strongest complexes with GT mismatches and single unpaired bases, whereas poor binding is observed at CC mismatches ($\Delta T > GT > CT > TT \approx CC \approx AT$) (33). The CC mismatch is little appeared to methyl-directed MMR in *Escherichia coli*.

In the present study, immobilized MutS on the gold electrode was used to detect the interaction between MutS and mismatched DNA by electrochemical methods including cyclic voltammetry (CV), EQCM and impedance. These label-free electrochemical methods have the advantage of simple and direct detection, exposing protein and DNA in more diverse environments than any other methods. Moreover, this protein immobilized sensor system is differentiated from the DNA probing methods for 'reusability' by an EDTA treatment. X-ray photoelectron spectroscopy (XPS) was used to confirm the interaction between MutS and the heteroduplex, and EQCM was used for quantitative analysis of MutS affinity with the heteroduplex.

## MATERIALS AND METHODS

### Materials

Sodium phosphate monobasic, sodium phosphate dibasic, sodium chloride, potassium chloride, nickel sulfate and ferricyanide were purchased from Sigma (USA). $N_6$-carbobenzyloxy-L-lysine, bromoacetic acid and 4-butyrothiolactone were purchased from Aldrich (USA).

### Expression and purification of proteins

Cloned *E.coli* MutS with an N-terminal His-tag in a pET15b vector over-expressed from the *E.coli* strain BL21 (DE3) (Novagene). After harvesting, the cells were suspended in 100 ml of lysis buffer (20 mM Tris–HCl, pH 8.0, 0.5 mM 2-mercaptoethanol, 1 μg/ml lysozyme and 250 μM phenylmethlysulfonyl fluoride), and lysed by sonication. The supernatant was applied to a 5 ml Hi-trap Ni-column (Amersham Pharmacia Biotech) pre-equilibrated with binding buffer (20 mM Tris–HCl, pH 8.0, 0.5 mM 2-mercaptoethanol and 500 mM NaCl). The column was washed with a 16% elution buffer and eluted with 300 mM imidazole. Protein was then applied to a MonoQ column (Amersham Pharmacia Biotech) equilibrated in buffer A (20 mM Tris–HCl, pH 8.0, 1 mM EDTA and 1 mM DTT) and eluted in buffer A with increasing NaCl concentration. MutS (150 μg/ml) was prepared for the further electrochemical experiment.

**Table 1.** DNA sequences used in this study

| Type | DNA sequence |
|---|---|
| AT homoduplex | 5′-GAC GAG CCG C**A**C GCT AGC GTC G |
| | 3′-CTG CTC GGC G**T**G CGA TCG CAG C |
| GT heteroduplex | 5′-GAC GAG CCG C**G**C GCT AGC GTC G |
| | 3′-CTG CTC GGC G**T**G CGA TCG CAG C |
| CT heteroduplex | 5′-GAC GAG CCG C**C**C GCT AGC GTC G |
| | 3′-CTG CTC GGC G**T**G CGA TCG CAG C |
| CC heteroduplex | 5′-GAC GAG CCG C**C**C GCT AGC GTC G |
| | 3′-CTG CTC GGC G**C**G CGA TCG CAG C |

Mismatched base pairs are presented in bold and underline.

### Hybridization of single-stranded DNA and purification of double-stranded DNA

Eight oligonucleotides were purchased from Bioneer, Inc. (Korea) for three different types of heteroduplex and one homoduplex (Table 1). These were annealed by incubation in 90°C water for 10 min and a decrease of the temperature to melting temperature for 3 h. The annealed double-strand DNA (dsDNA) was purified using a reverse-phase chromatography column. All dsDNA concentrations were determined at $UV_{260}$. DNA solutions (2, 6 and 10 μM) in the phosphate buffer (pH 7.4) were prepared for the electrochemical experiment.

### Synthesis of HS-NTA

(1*S*)-*N*-[5-[(4-Mercaptobutanoyl)amino]-1-carboxypentyl] iminodiacetic acid (HS-NTA) was synthesized from $N_6$-Carbobenzyloxy-L-lysine as reported previously (34). The product was characterized with elemental analysis, FT-IR and NMR spectroscopy (data not shown).

### Electrochemical and XPS measurements

A conventional three-electrode system was used. The reference electrode was constructed by sealing an Ag/AgCl wire into a glass tube with a solution of 3.0 M KCl and capped with a Vycor tip. The counter electrode was a platinum wire. Protein modified electrodes were used as working electrodes. All experiments were conducted at room temperature. CV was measured using a Potentiostat/Galvanostat Kosentech Model KST-P1 (Korea). Impedance spectra were collected using PARSTAT 2263 (USA) at an open circuit voltage of 100 KHz down to 100 mHz (AC amplitude, 10 mV; sampling rate, 10 points per decade). The quantity of immobilized molecules including protein and DNA were determined with an EQCM analyzer (QCM 100 from Stanford Research Systems, USA). The working electrode for the EQCM experiments was a 5 MHz AT-cut quartz crystal with a gold electrode. The diameter of the quartz crystal was 13.7 mm and the gold electrode diameter was

5 mm. CVs and impedance spectra were recorded in a phosphate buffer (100 mM NaCl, 50 mM KCl and 20 mM phosphate, pH 7.4) with 5 mM $Fe(CN)_6^{3-}$. EQCM experiments were carried out in a phosphate buffer (100 mM NaCl, 50 mM KCl and 20 mM phosphate, pH 7.4). ESCA experiments were performed using a VG scientific ESCA lab 250 XPS spectrometer with a monochromated AlKα source with charge compensation in the Korea Basic Science Institute (Busan).

Gold disk electrodes (~0.02 $cm^2$ geometrical area) were used for the electrochemical measurements. Before modification of the gold electrodes, they were polished to a mirror finish with 0.05 μm alumina, and then sonicated for 60 s in alcohol and distilled water, respectively. Then, the electrochemical pretreatments were performed by cycling from a potential of −0.8 to +1.3 V versus Ag/AgCl in a 0.1 M $H_2SO_4$ solution.

### Immobilization of MutS

The freshly cleaned gold electrode was incubated in 10 mM HS-NTA for 1 h at room temperature and 120 r.p.m. on a shaker. The HS-NTA coated electrode was immersed in a 100 mM $NiSO_4$ solution for 10 min. The Ni-NTA coated electrode was rinsed with phosphate buffer and subsequently incubated in 150 μg/ml N-terminal his tagged MutS for 15 min. The final MutS probe deposited for 20 min was rinsed with phosphate buffer to remove the weakly absorbed protein. The immobilization of the protein on the electrode was confirmed by CV, XPS, EQCM and impedance techniques.

### Analytical procedures

The MutS probe was dipped into a phosphate buffer containing various types of heteroduplexes or one homoduplex at room temperature for 15 min, then rinsed with phosphate buffer to remove unbound DNA. The electrochemical evaluation for the specific binding behavior of heteroduplexes towards the MutS modified electrode was performed in a measuring solution containing ferricyanide ion.

The change of electrochemical signal by CV and impedance was also detected in the measuring solution containing ferricyanide ions. The impedance measurement was also carried out after treating the DNA modified electrode with 100 mM EDTA for 4 h in order to check the recycle ability.

## RESULTS AND DISCUSSION

### Immobilization of MutS on the electrode

To fabricate the probe of MutS immobilized on the electrode surface, mediators were required. The gold electrode was coated with HS-NTA by the formation of linkage between Au and a thiol group. $Ni^{2+}$ was bound to three carboxyl groups and one nitrogen of HS-NTA by formation of chelating bonds. His-tag MutS was combined into $Ni^{2+}$ on the electrode using the strong affinity between histidine and $Ni^{2+}$ (Figure 1). The state of the probe could be detected indirectly according to the bound type and amount of material through observation of the change of redox peaks of $Fe(CN)_6^{3-}$ in CV. CV measurements (potential, 0.6 to

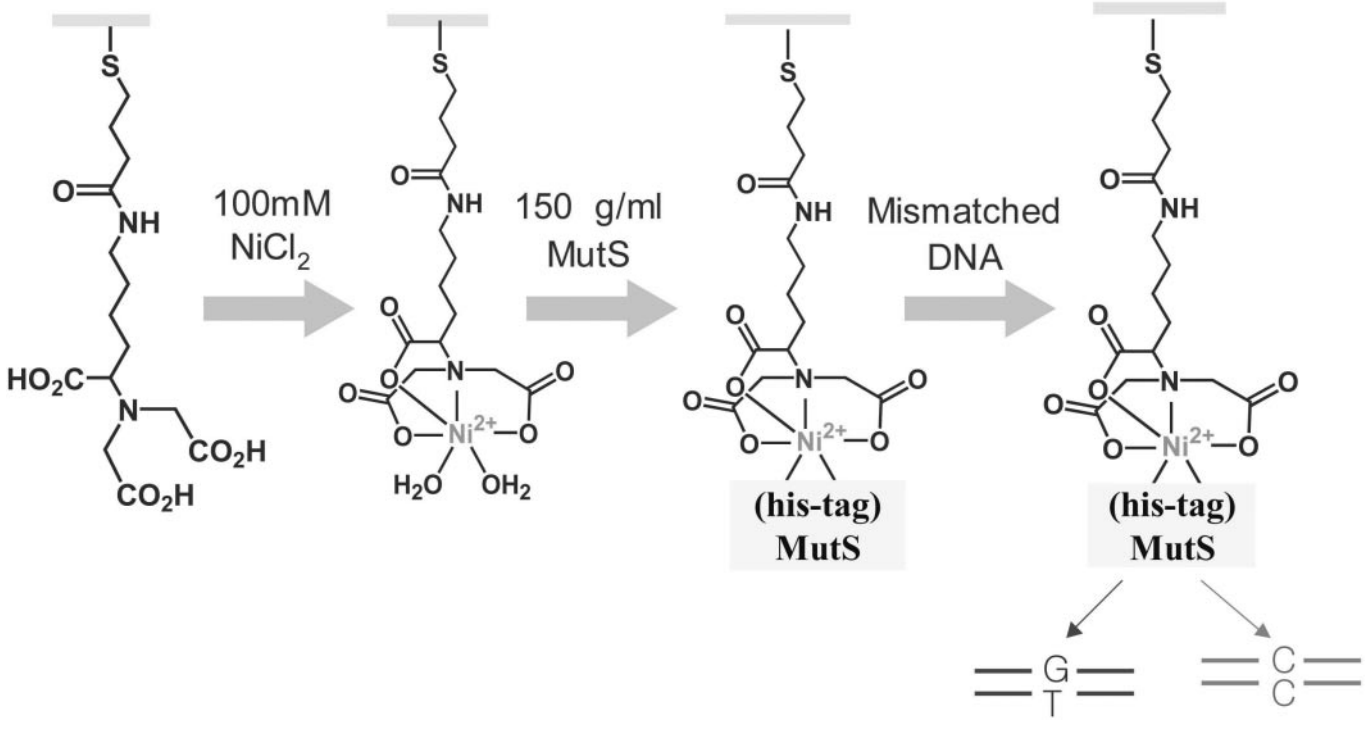


**Figure 1.** A schematic representation for the detection of interaction between immobilized MutS and DNA. The HS-NTA coated gold electrode was immersed in $NiSO_4$ solution. The Ni-NTA coated electrode immobilized with the protein and MutS modified electrode was reacted with various types of heteroduplex and one homoduplex for the electrochemical analysis.

−0.2 V; scan rate, 100 mV/s) were carried out in phosphate buffer containing 5 mM $Fe(CN)_6^{3-}$. As shown in Figure 2A, the redox peak current of ferricyanide marker ions [$Fe(CN)_6^{3-}$] was significantly lowered by immobilization of the negatively charged HS-NTA on the gold electrode. Because the compactly coated HS-NTA on the electrode have negatively charged carboxylate groups, the electrochemical diffusion of redox anions was blocked towards the

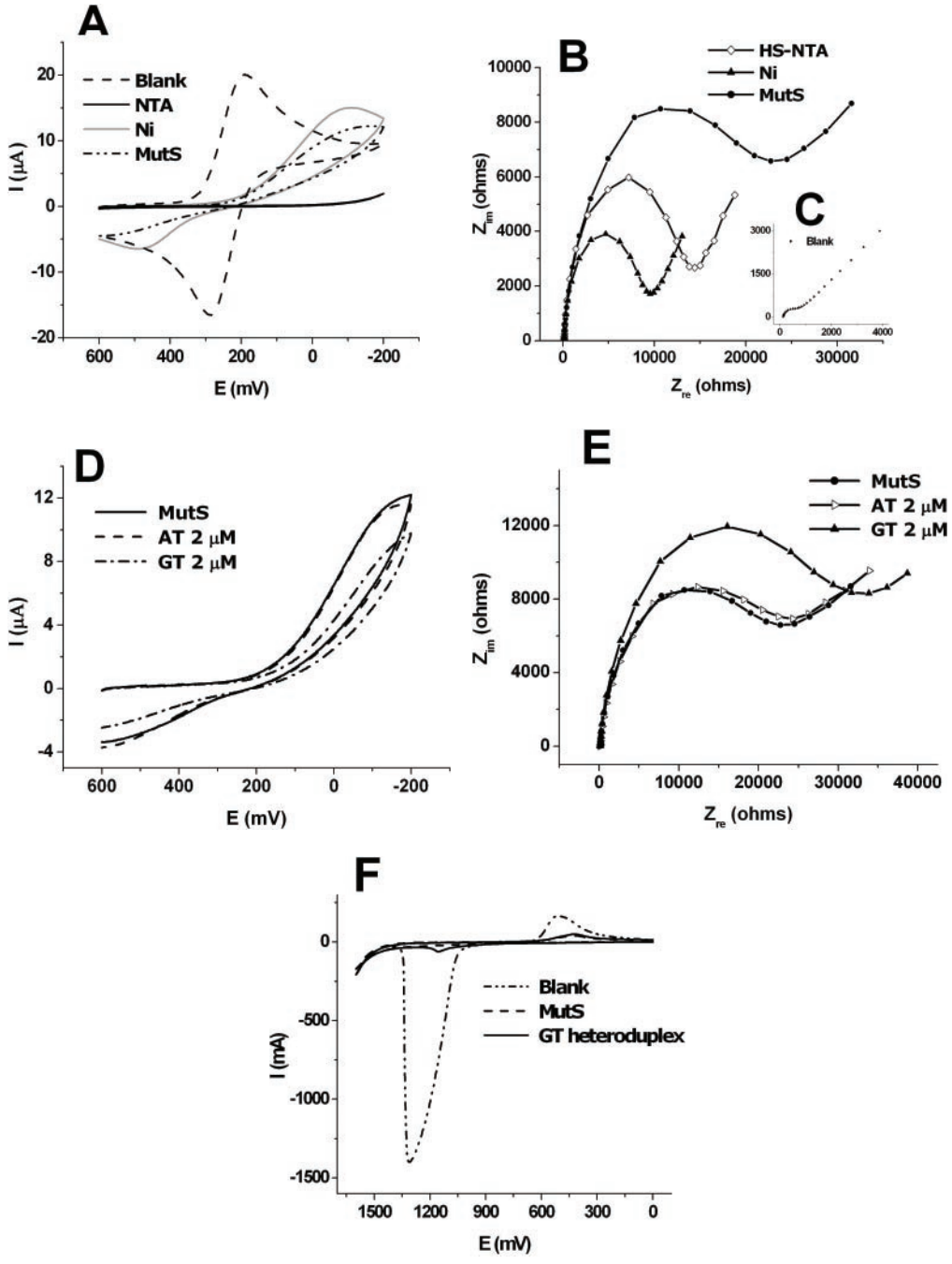


**Figure 2.** (**A**) Cyclic voltammogram for blank, HS-NTA coated step, Ni-NTA coated step and MutS immobilized step in the presence of 5 mM $Fe(CN)_6^{3-}$. Indirect detection of the state of electrode was possible through observation of the change of redox peaks in CV. (**B**) Nyquist plots for each immobilized step, HS-NTA coated step (open diamond), Ni-NTA-HS coated step (closed triangle), MutS immobilized step (closed circle). After immobilization of HS-NTA, $R_{ct}$ is increased (open diamond), then formation of Ni-NTA complex causes a decrease of $R_{ct}$. After immobilization of protein, $R_{ct}$ is re-increased due to interference degree of $Fe(CN)_6^{3-}$ for the condition of electrode surface. (**C**) Blank in the presence of 5 mM $Fe(CN)_6^{3-}$. (**D**) Cyclic voltammogram and (**E**) Nyquist plots measured after the reaction of AT homoduplex and GT heteroduplex. The CV and impedance results shown in (D) and (E) are the specific interaction between MutS and heteroduplex (dash-dot line and closed triangle line), whereas indicated little change between MutS and homoduplex (dashed line and open triangle line). (**F**) Differential pulse voltammograms measured at 0 to +1.6 V before and after the reaction of GT heteroduplex. Differential pulse voltammetry (DPV) was used to observe the oxidation peak of adenines of the dsDNA captured by MutS after interaction of the MutS probe with GT heteroduplex.

electrode surface due to the electrostatic repulsion. Since the HS-NTA has three anions within one molecule, the access of $Fe(CN)_6^{3-}$ to the electrode surface to reveal the electrochemical reaction is more fully blocked. After $Ni^{2+}$ binds to a HS-NTA modified electrode, the redox peak of $Fe(CN)_6^{3-}$ was somewhat increased. It is possible that $Ni^{2+}$ ions make a moving of $Fe(CN)_6^{3-}$ to the electrode surface, and the approaching of $Fe(CN)_6^{3-}$ to the surface is easier due to electrostatic attraction between cationic metal ions and anionic marker ions. On the other hand, the immobilization of MutS on the HS-NTA/$Ni^{2+}$ layer causes a decrease in the redox peak current of $Fe(CN)_6^{3-}$, because of steric hindrance of the huge protein of MutS on the electrode surface.

To confirm the CV results, impedance (frequency range, 100 kHz to 100 mHz; AC amplitude, 10 mV) was measured for individual steps in a phosphate buffer solution containing 5.0 mM $Fe(CN)_6^{3-}$ at room temperature. When the specific material binds to the electrode, a change of the electrochemical properties of the electrode occurs. The change in charge transfer resistance ($R_{ct}$) determined from the diameter of the semicircle in the Nyquist plot reflects the interference to the effective moving of $Fe(CN)_6^{3-}$ ions to the electrode surface according to the state of the surface. Figure 2B shows the Nyquist plot of impedance obtained after immobilization of each step of HS-NTA and $Ni^{2+}$, and MutS in comparison with a blank (Figure 2C). After immobilization of HS-NTA on the electrode, $R_{ct}$ is greatly increased. The formation of the Ni-NTA complex causes a decrease of $R_{ct}$, and the immobilization of MutS leads to an increase of $R_{ct}$. Thus, results of CV and impedance experiments suggested that Histidine tagged MutS was successfully immobilized on the modified gold electrode with Ni-NTA.

### Interaction between MutS and heteroduplexes

To examine the interaction between the MutS probe and heteroduplexes, it was incubated in a 2 μM solution (phosphate buffer) of heteroduplex containing GT mismatched pairs for 15 min at room temperature. In order to compare the difference of the affinity of MutS between heteroduplex and homoduplex, the probe was incubated in 2 μM solution of homoduplex containing AT matched pairs instead of GT heteroduplex for 15 min. Figure 2D shows the CV results obtained before and after the reaction with homoduplex and heteroduplex. The electrochemical response showed nearly no change in the case of reaction with homoduplex. However, there was a significant reduction of the peak current of redox marker ions observed in the case of the reaction with heteroduplex, owing to electrostatic repulsions between anionic marker ions and polyanionic DNA duplexes which were accumulated on the probe.

To confirm the CV results, impedance was measured before and after the reaction with homoduplex and heteroduplex. Figure 2E shows the specific interaction between MutS and heteroduplex. After incubating in GT heteroduplex, the $R_{ct}$ values were increased due to the blocking behavior of marker ions. However, there was no difference in $R_{ct}$ values before and after the reaction with homoduplex. In addition, the heteroduplex interaction with MutS on the electrode was confirmed by observation of the oxidation peak of DNA. Figure 2F shows the DPV results, obtained for the MutS probe and the probe capturing GT heteroduplex. After interaction of the MutS probe with heteroduplex, the anodic peak appeared at 1.15 V, which corresponds to the oxidation peak of the adenines of the dsDNA captured by MutS.

In addition, these results were also confirmed with XPS analysis. Figure 3A shows the survey spectra for the HS-NTA modified gold electrode surface. The presence of C1s, N1s and O1s peaks for the HS-NTA modified electrode surface clearly shows that a SAM (Self Assembly Monolayer) layer of HS-NTA was formed on the Au electrode surface. The presence of Ni 2p3 and Ni 2p1 peaks in the spectrum (Figure 3B, curve a) shows that $Ni^{2+}$ was chelated with the HS-NTA molecules (35). Moreover, the N1s and O1s peaks at 399.7 and 531.9 eV, respectively, shifted to the higher energy at 400.5 and 532.6 eV after $Ni^{2+}$ binding with HS-NTA confirms the $Ni^{2+}$ binding with the HS-NTA modified surface. Figure 3B, curve b shows the XPS survey spectrum obtained after the immobilization of MutS. The N1s and O1s peaks at 400.5 and 532.6 eV in the Ni-NTA modified electrode shifted to the higher energy of 402.5 and 535.5 eV, respectively. The intensity of the N1s peak was also increased, indicating that the protein was successfully immobilized on the Ni-NTA surface. In addition, the shift of N1s, O1s and Ni2p3 peaks to higher energy indicates that the His-tagged protein was immobilized on the NTA-Ni surface. Figure 3B, curve c shows the XPS survey spectrum

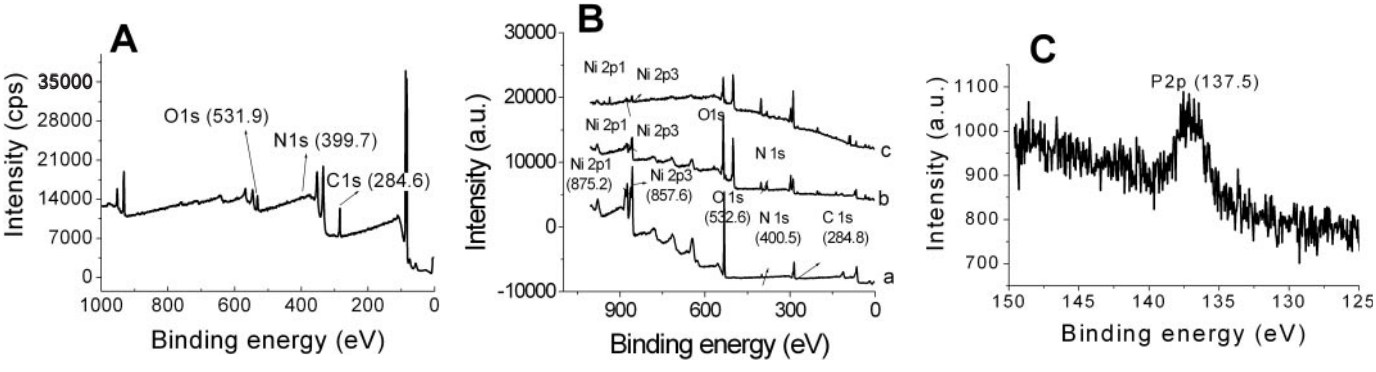


**Figure 3.** XPS survey spectra of (**A**) NTA modified Au electrode, (**B**) Ni-NTA (curve a), MutS-Ni-NTA (curve b) and DNA-MutS-Ni-NTA (curve c) modified Au electrodes (**C**) P2p peak obtained after DNA interaction with a protein immobilized Ni-NTA surface.

of a MutS-Ni-NTA surface after interaction with DNA. The C1s, N1s, O1s and Ni2p peaks did not change, after the interaction of DNA. It is expected that DNA covered the Ni-NTA-MutS surface, thus, the C1s, N1s, O1s and Ni2p peaks did not shift. Figure 3C shows a P2p peak at 137.45 eV in the heteroduplex-modified electrode, which confirms that the DNA interacted with the MutS-Ni-NTA surface.

### MutS affinity according to heteroduplex types

To examine MutS affinity to heteroduplex types containing different mismatched pairs, after the MutS probe was separately incubated in the GT, CT and CC heteroduplex solutions (2, 6, 10 μM) for 15 min at room temperature. Figure 4A–C shows CVs recorded before and after binding with GT, CT

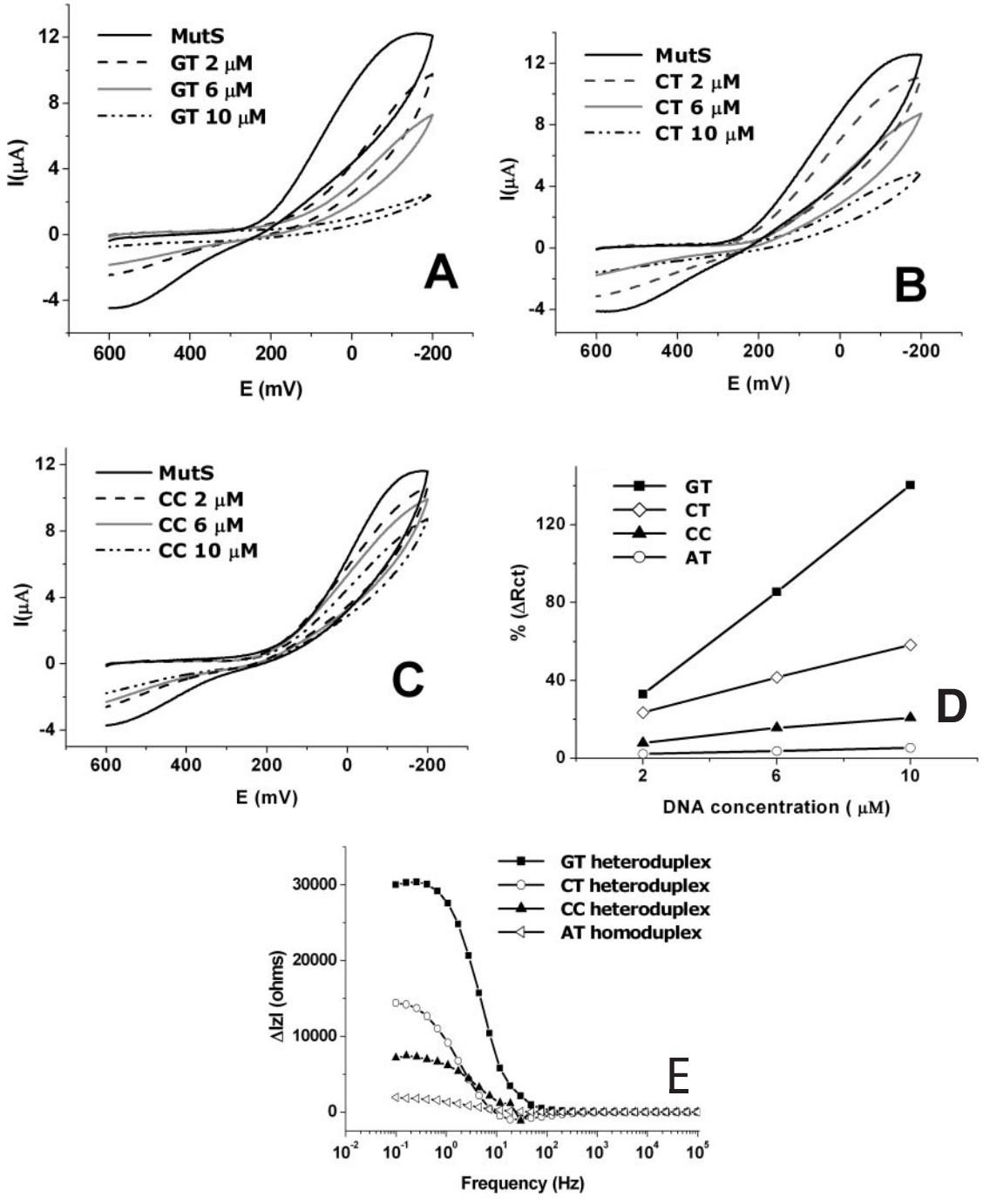


**Figure 4.** Cyclic voltammogram measured before and after the reaction of (**A**) GT heteroduplex (2, 6 and 10 μM), (**B**) CT heteroduplex (2, 6 and 10 μM) and (**C**) CC heteroduplex (2, 6 and 10 μM). In (A–C), MutS affinity to heteroduplex types is dependent on concentration. (**D**) The MutS affinity to heteroduplex and homoduplex at concentrations. $\%\Delta R_{ct}$s are represented increased charge transfer resistance after interaction with dsDNA/charge transfer resistance of MutS × 100. (**E**) The difference of the bode plot measured before and after binding with 10 μM heteroduplex and homoduplex. The results indicate that MutS has different binding affinities to GT, CT and CC heteroduplexes. The order of binding affinity of MutS is GT > CT > CC > AT.

**Table 2.** $R_{ct}$ values[a], $R_{ct}$ change values and change ratio of $R_{ct}$ values before and after interaction MutS with heteroduplex and homoduplex

| | GT | CT | CC | AT |
|---|---|---|---|---|
| $R_{ct}$ (Ω) | | | | |
| MutS | $(2.43 \pm 0.51) \times 10^4$ | $(3.06 \pm 0.43) \times 10^4$ | $(3.82 \pm 0.68) \times 10^4$ | $(3.78 \pm 0.70) \times 10^4$ |
| 2 μM | $(3.24 \pm 0.23) \times 10^4$ | $(3.78 \pm 0.18) \times 10^4$ | $(4.12 \pm 0.27) \times 10^4$ | $(3.87 \pm 0.15) \times 10^4$ |
| 6 μM | $(4.52 \pm 0.31) \times 10^4$ | $(4.34 \pm 0.25) \times 10^4$ | $(4.42 \pm 0.29) \times 10^4$ | $(3.22 \pm 0.17) \times 10^4$ |
| 10 μM | $(5.86 \pm 0.36) \times 10^4$ | $(4.85 \pm 0.24) \times 10^4$ | $(4.92 \pm 0.25) \times 10^4$ | $(3.98 \pm 0.19) \times 10^4$ |
| $\Delta R_{ct}$ (Ω) | | | | |
| 2 μM | 8050 | 7190 | 3000 | 860 |
| 6 μM | 20 810 | 12 730 | 6000 | 1410 |
| 10 μM | 34 200 | 17 870 | 11 020 | 2030 |
| $\%(\Delta R_{ct})$ | | | | |
| 2 μM | 33 | 23 | 8 | 2 |
| 6 μM | 85 | 41 | 16 | 4 |
| 10 μM | 140 | 58 | 21 | 6 |
| Detection limit[b] (μM) | 0.044 | 0.13 | 0.31 | 1.56 |

[a]The values of $R_{ct}$ are mean ± SD of three repeated experiments.
[b]Detection limit $C_m = (S_m - \bar{S}_{bl})/m$, $S_m = \bar{S}_{bl} + ks_{bl}$ ($\bar{S}_{bl}$, mean of blank; $S_{bl}$, standard deviation of blank; $k$, detection limit constant, blank contains only the MutS solution).

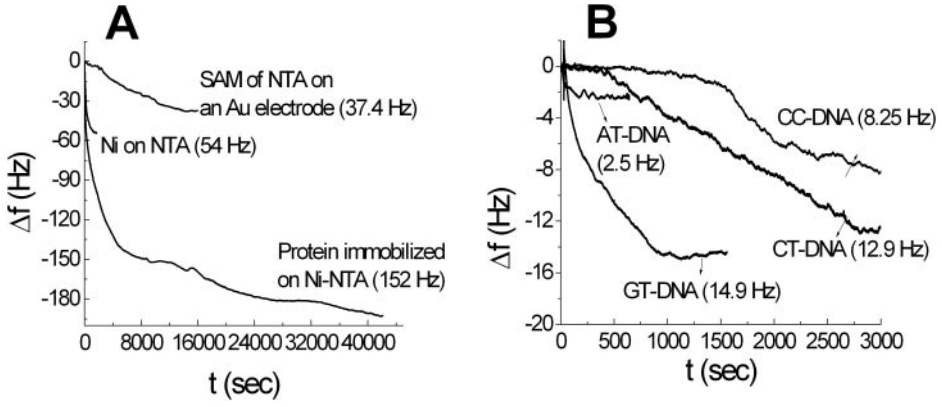


**Figure 5.** EQCM experiments for (**A**) each immobilized step, HS-NTA coated step, Ni-NTA-HS coated step, MutS immobilized step, and (**B**) DNA interaction with the protein modified NTA-Ni surface.

and CC heteroduplexes. In the case of GT heteroduplex (Figure 4A), a significant decrease of the redox peak of marker ions was observed, indicating that the amount of dsDNA was increased on the electrode due to the strong affinity to MutS. The next highest affinity to MutS was shown by CT heteroduplex (Figure 4B), and a weak binding of MutS was observed to the CC heteroduplex (Figure 4C). The affinity of MutS to the AT homoduplex was observed with a little change (data not shown).

To confirm CV results, impedance was measured before and after binding with GT, CT and CC heteroduplexes and AT homoduplex. Table 2 shows the $R_{ct}$ values and $R_{ct}$ change values from MutS to the dsDNA in the Nyquist plot before and after interaction with GT, CT and CC heteroduplexes and the AT homoduplex. The change ratio of $R_{ct}$ values (increased charge transfer resistance after interaction with dsDNA/charge transfer resistance of MutS × 100: %ΔlZl) from MutS to the dsDNA is also calculated. $R_{ct}$ values were sensitive to the condition of the electrode surface, so a small change appeared in spite of reaction they executed in the same concentration and at the same time. The change ratios of $R_{ct}$ values were obtained from average $R_{ct}$ value of three repeated experiments. Based on these data, calibration curves of $R_{ct}$ according to the concentrations of heteroduplexes and homoduplex were investigated. In GT heteroduplex case, the slope was $3.376 \times 10^3$ Ω/cm ($r^2 = 0.99$) with detection limit of 44 nM. In CT heteroduplex, CC heteroduplex and AT homoduplex cases, the slope were

**Table 3.** Mass change values of EQCM experiments

| | Mass (μg/cm$^2$) | Number of mols (mol/cm$^2$) | Number of molecules (molecules/cm$^2$) |
|---|---|---|---|
| (A) Each immobilized step | | | |
| SAM of NTA | 0.5 | $2 \times 10^{-9}$ | $1.2 \times 10^{15}$ |
| Ni-NTA | 0.76 | $1.3 \times 10^{-8}$ | $7.8 \times 10^{15}$ |
| Protein-Ni-NTA | 2.7 | $2.84 \times 10^{-11}$ | $1.71 \times 10^{13}$ |
| (B) Different types of DNA | | | |
| GT heteroduplex | 0.2 | $1.5 \times 10^{-11}$ | $9.2 \times 10^{12}$ |
| CT heteroduplex | 0.18 | $1.3 \times 10^{-11}$ | $8.0 \times 10^{12}$ |
| CC heteroduplex | 0.11 | $8.3 \times 10^{-12}$ | $5.1 \times 10^{12}$ |
| AT homoduplex | 0.035 | $2.6 \times 10^{-12}$ | $1.6 \times 10^{12}$ |

After immobilization of MutS, large difference of mass change was observed due to MutS protein with large molecular weight (~95 kDa). In addition, the order of interaction is GT > CT > CC > AT with the same results in the case of CV and impedance according to mass change of DNA appeared in (A).

**Table 4.** Change value of $R_{ct}$ of each step before and after treatment of 100 mM EDTA and change ratio of $R_{ct}$ after binding GT heteroduplex

| | HS-NTA | $Ni^{2+}$ | MutS | GT 2 μM |
|---|---|---|---|---|
| Experiment 1 $R_{ct}$ (Ω) | $(1.43 \pm 0.10) \times 10^4$ | $(9.09 \pm 0.08) \times 10^3$ | $(2.43 \pm 0.51) \times 10^4$<br>%($\Delta R_{ct}$): 33% | $(3.24 \pm 0.23) \times 10^4$ |
| Treatment of 100 mM EDTA for 4 h | | | | |
| Experiment 2 $R_{ct}$ (Ω) | $(1.09 \pm 0.23) \times 10^4$ | $(7.95 \pm 0.07) \times 10^3$ | $(2.89 \pm 0.47) \times 10^4$<br>%($\Delta R_{ct}$): 35% | $(3.90 \pm 0.32) \times 10^4$ |

After treatment of EDTA on the GT heteroduplex modified electrode, nearly same value of the change ratio of $R_{ct}$ was appeared. Values in the table are the mean ± SD of three repeated experiments.

each $1.684 \times 10^3$ Ω/cm ($r^2 = 0.95$), $1.052 \times 10^3$ Ω/cm ($r^2 = 0.98$) and $0.18 \times 10^3$ Ω/cm ($r^2 = 0.94$) with detection limit of 0.13, 0.31 and 1.56 μM, respectively (calibration curves are not shown). These detection limits are comparable with the results of the label-free SPR method (36).

Figure 4D shows the change ratios of $R_{ct}$. The larger association of the heteroduplex to the MutS probe is accompanied by a significant increase in change ratios of $R_{ct}$ and a steep gradient according to the DNA concentration. Figure 4E shows the difference of the impedance values (ΔlZl) of the MutS probe before and after reacting with individual 10 μM GT, CT and CC heteroduplex in a bode plot. The largest difference in impedance values ($\Delta lZl_{max}$) of the MutS probe before and after binding with individual GT, CT and CC heteroduplexes was obtained at ~300 mHz. In the case of the GT heteroduplex, $\Delta lZl_{max}$ was the greatest of all the dsDNAs. Whereas, in the case of the CC heteroduplex, there was a small change in the value of $\Delta lZl_{max}$, indicating the weak affinity of MutS to the CC heteroduplex. The affinity order of MutS for the dsDNAs was GT > CT > CC > AT. These results show that MutS has different binding affinities to GT, CT and CC heteroduplexes with a similar preference to previous electrophoretic mobility shift assay results (GT > CT > CC ≈ AT). The results of CV and impedance clearly show that the interaction of MutS with the CC heteroduplex is much stronger than that with AT homoduplex.

In order to show the affinity of MutS to heteroduplexes quantitatively, EQCM analysis was also carried out using the MutS probe. Figure 5A shows the frequency versus time curves obtained during the preparation of the SAM of NTA on a gold electrode, complexation between $Ni^{2+}$ and NTA molecules, and protein immobilization on the Ni-NTA surface. During the preparation of the SAM, the frequency decreased and reached a steady state after 5 h. This means that the monolayer formation of NTA was completed within 5 h. After 5 h, the frequency decrease was observed to be 37.4 Hz. During the binding of Ni (II) with the SAM of NTA, the frequency decreased very rapidly and it reached steady state within 30 min. This means that the chelation of the Ni (II) ion with NTA proceeds faster than the SAM formation. The frequency decrease was observed to be 54 Hz. During the immobilization of protein, the frequency rapidly decreased and reached a steady state after 4 h. The frequency continued to decrease as time passed, although the frequency did not significantly changed from 4 to 11 h immobilization time. The frequency decreased after 11 h was found to be 193 Hz. The mass changes were determined from the change in frequency following the previous study (10) using the Sauerbrey equation (37):

$$\Delta m = (-1/2)(f_0^{-2})(\Delta f)A(k\rho)^{1/2},$$

where, $\Delta m$ is the mass change, $\Delta f$ is the observed frequency change, $A$ is the area of the gold disk coated onto the quartz crystal, ρ is the density of the crystal, $k$ is the shear modulus of the crystal, $f_0$ is the oscillation frequency of the crystal. The mass changes, number of moles and number of molecules are shown in Table 3A. The interactions of different types of DNA with the protein immobilized Ni-NTA surface were also investigated. Figure 5B shows the frequency versus time curves obtained during the interactions of different types of DNA with the protein immobilized on the Ni-NTA surface. For CC, CT and GT heteroduplexes, the frequency decrease attained a steady state within 1 h. The frequencies that changed after 1 h interaction were found to be 8.25, 12.5 and 14.9 Hz, respectively. For the AT homoduplex, the frequency shift attained a steady state within 5 min. The mass change, number of moles and number of molecules of different types of DNA–protein interactions are shown in Table 3(B). By measuring the MutS-binding signal on the DNA probe immobilized electrode in EQCM analysis, heteroduplexes have been discriminated from the homoduplex down to a target concentration of 1 nM (28). Using the MutS probe, the detection limit was increased because the relative mass change of DNA is smaller than that of protein. The order of interaction is GT > CT > CC > AT with the same results in the case of CV and impedance. Thus, the CV and impedance results clearly show that MutS can distinguish between the CC heteroduplex and the AT homoduplex with different affinities.

## Reusability of the probe

The immobilized His-tag protein on the electrode surface can be refreshed through formation of stronger binding between EDTA and Ni ions. To examine the applicability of recyclable sensors, after the GT heteroduplex modified electrode was incubated in a 100 mM EDTA solution for 4 h at room temperature, this electrode was incubated subsequently in $Ni^{2+}$ and MutS solutions. The MutS re-immobilized electrode was incubated in 2 μM GT heteroduplex solution. Table 4 shows the change in values of $R_{ct}$ of each step and the change in ratios of $R_{ct}$ from MutS to the GT heteroduplex. After treating the GT heteroduplex captured probe with EDTA, a similar value of $R_{ct}$ compared to the HS-NTA modified electrode is observed. In addition, the change in ratio of $R_{ct}$ from MutS to GT heteroduplex after processing with EDTA

is analogous to that before the processing with EDTA, indicating that this biosensor can be recyclable.

## CONCLUSION

In this study, electrochemical detection of the interaction between MutS and mismatched DNA using CV and impedance methods has been demonstrated. In CV experiments, the more the redox peak of $Fe(CN)_6^{3-}$ decreased, the more the MutS probe with mismatched DNA (heteroduplex) interacted. In impedance results, the more $R_{ct}$ increased, the greater the MutS–mismatched DNA interaction. This also confirms that MutS has different binding affinities to the mismatched DNA (GT > CT > CC > AT). These results clearly show that the interaction of MutS with the CC heteroduplex is much higher than that with AT homoduplex. EQCM results quantified these affinities. This direct methodological approach can be widely applicable for detecting the interaction between various proteins and their targets.

## ACKNOWLEDGEMENTS

The authors gratefully acknowledge financial supports from the Center for Integrated Molecular Systems at POSTECH (R11-2000-070-070010), the Basic Research program of the KOSEF (R01-2004-000-10210-0) and Korea Health Industry Development Institute through Healthcare and Biotechnology Development Program (A050426). Funding to pay the Open Access publication charges for this article was provided by Pohang University of Science and Technology.

*Conflict of interest statement*. None declared.

## REFERENCES

1. Patikoglou,G. and Burley,S.K. (1997) Eukaryotic transcription factor–DNA complexes. *Annu. Rev. Biophys. Biomol. Struct.*, **26**, 289–325.
2. Modrich,P. and Lahue,R. (1996) Mismatch repair in replication fidelity, genetic recombination, and cancerbiology. *Annu. Rev. Biochem.*, **65**, 101–133.
3. Schofield,M.J., Nayak,S., Scott,T.H., Du,C. and Hsieh,P. (2001) Interaction of *Escherichia coli* MutS and MutL at a DNA mismatch. *J. Biol. Chem.*, **276**, 28291–28299.
4. Smith,J. and Modrich,P. (1996) Mutation detection with MutH, MutL, and MutS mismatch repair proteins. *Proc. Natl Acad. Sci. USA*, **93**, 4374–4379.
5. Lishanski,A., Ostrander,E.A. and Rine,J. (1994) Mutation detection by mismatch binding protein, MutS, in amplified DNA: application to the cystic fibrosis gene. *Proc. Natl Acad. Sci. USA*, **91**, 2674–2678.
6. Galas,D.J. and Schmitz,A. (1978) A DNA footprinting: a simple method for the detection of protein–DNA binding specificity. *Nucleic Acids Res.*, **5**, 3157–3170.
7. Palecek,E., Fojta,M., Tomschick,M. and Wang,J. (1998) Electrochemical biosensors for DNA hybridization and DNA damage. *Biosens. Bioelectron.*, **13**, 621–628.
8. Cahova-Kucharıkova,K., Fojta,M., Mozga,T. and Palecek,E. (2005) Use of DNA repair enzymes in electrochemical detection of damage to DNA bases *in vitro* and in cells. *Anal. Chem.*, **77**, 2920–2927.
9. Palecek,E. and Jelen,F. (2002) Electrochemistry of nucleic acids and development of DNA sensors. *Crit. Rev. Anal. Chem.*, **3**, 261–270.
10. Lee,T.-Y. and Shim,Y.-B. (2001) Direct DNA hybridization detection based on the oligonucleotide-functionalized conductive polymer. *Anal. Chem.*, **73**, 5629–5632.
11. Darain,F., Ban,C. and Shim,Y.-B. (2004) Development of a new and simple method for the detection of histdine-tagged proteins. *Biosens. Bioelectron.*, **20**, 857–863.
12. Rahman,M.A., Kwon,N.-H., Won,M.-S., Choe,E.S. and Shim,Y.-B. (2005) Functionalized conducting polymer as an enzyme-immobilizing substrate: an amperometric glutamate microbiosensor for *in vivo* measurements. *Anal. Chem.*, **77**, 4854–4860.
13. Ban,C., Chung,S., Park,D. and Shim,Y.-B. (2004) Detection of protein–DNA interaction with a DNA probe: distinction between single-strand and double-strand DNA–protein interaction. *Nucleic Acids Res.*, **32**, e110/1–e110/8.
14. Strasak,L., Dvorak,J., Hason,S. and Vetterl,V. (2002) Electrochemical impedance spectroscopy of polynucleotide adsorption. *Bioelectrochemistry*, **56**, 37–41.
15. Hason,S., Dvorak,J., Felen,F. and Vetterl,V. (2002) Impedance analysis of DNA and DNA–drug interactions on thin mercury film electrodes. *Crit. Rev. Anal. Chem.*, **32**, 167–169.
16. Vetterl,V., Papadopoulos,N., Drazan,V., Strasak,L., Hason,S. and Dvorak,J. (2000) Nucleic acid sensing by impedance measurements. *Electrochem. Acta*, **45**, 2961–2971.
17. Palecek,E., Fojta,M., Jelen,F. and Vetterl,V. (2002) Electrochemical analysis of nucleic acids. In Bard,C.A. and Stratman,S. (eds), *Encyclopedia of Electrochemistry*. In Wilson,G.S. (ed.), *Bioelectrochemistry*. Wiley-VCH Verlag, Weinheim**,** Vol. **9**, pp. 365–430.
18. Darain,F., Park,D.-S., Park,J.-S., Chang,S.-C. and Shim,Y.-B. (2005) A separation-free amperometric immunosensor for vitellogenin based on screen-printed carbon arrays modified with a conductive polymer. *Biosens. Bioelectron.*, **20**, 1780–1787.
19. Ge,B., Scheller,F.W. and Lisdat,F. (2003) Electrochemistry of immobilized CuZnSOD and FeSOD and their interaction with superoxide radicals. *Biosens. Bioelectron.*, **18**, 295–302.
20. Wang,M., Wang,L., Wang,G., Ji,X., Bai,Y., Li,T., Gong,S. and Li,J. (2004) Application of impedance spectroscopy for monitoring colloid Au-enhanced antibody immobilization and antibody-antigen reactions. *Biosens. Bioelectron.*, **19**, 575–582.
21. Lu,A.L., Clark,S. and Modrich,P. (1983) Methyl-directed repair of DNA base-pair mismatches *in vitro*. *Proc. Natl Acad. Sci. USA*, **80**, 4639–4643.
22. Lieb,M. (1987) Bacterial genes MutL, MutS, and DCM participate in repair of mismatches at 5-methylcytosine sites. *J. Bacteriol.*, **169**, 5241–5246.
23. Schofield,M.J. and Hsieh,P. (2003) DNA mismatch repair; molecular mechanisms and biological function. *Annu. Rev. Microbiol.*, **57**, 579–608.
24. Han,A., Shibata,T., Takarada,T. and Maeda,M. (2002) Gene mutation assay using a MutS protein-modified electrode. *Nucleic Acids Res. Suppl.*, **2**, 287–288.
25. Li,C.-Z., Long,Y.-T., Lee,J.S. and Kraatz,H.-B. (2004) Protein–DNA interaction: impedance study of MutS binding to a DNA mismatch. *Chem. Commun.*, **5**, 574–575.
26. Gotoh,M., Hasebe,M., Ohira,T., Hasegawa,Y., Shinohara,Y., Sota,H., Nakao,J. and Tosu,M. (1997) Rapid method for detection of point mutations using mismatch binding protein (MutS) and an optical biosensor. *Genet. Anal.*, **14**, 47–50.
27. Babic,I., Andrew,S.E. and Firik,F.R. (1996) MutS interaction with mismatch and alkylated base containing DNA molecules detected by optical biosensor. *Mutat. Res.*, **372**, 87–96.
28. Su,X., Robelek,R., Wu,Y., Wang,G. and Knoll,W. (2004) Detection of point mutation and insertion mutations in DNA using a quartz crystal microbalance and MutS, a mismatch binding protein. *Anal. Chem.*, **76**, 489–494.
29. Kramer,B., Kramer,W. and Fritz,H.J. (1984) Different base–base mismatches are corrected with different efficiencies by the methyl-directed DNA mismatch-repair system of *Escherichia coli*. *Cell*, **38**, 879–887.
30. Dohet,C., Wagner,R. and Radman,M. (1985) Repair of defined single base-repair mismatches in *Escherichia coli*. *Proc. Natl Acad. Sci. USA*, **82**, 503–505.
31. Fazakerley,G.V., Quignard,E., Woisard,A., Guschlbauer,W., van der Marel,G.A., van Boom,J.H., Jones,M. and Radman,M. (1986) Structures of mismatched base pairs in DNA and their recognition by the *Escherichia coli* mismatch repair system. *EMBO J.*, **5**, 3697–3703.
32. Su,S.S., Lahue,R.S., Au,K.G. and Modrich,P. (1988) Mispair specificity of methyl-directed DNA mismatch correction *in vitro*. *J. Biol. Chem.*, **263**, 6829–6835.

33. Brown,J., Brown,T. and Fox,K.R. (2001) Affinity of mismatch binding protein MutS for heterodulexes containing different mismatches. *Biochem. J*., **354**, 627–633.
34. Roure,O.D., Debiemm-Chouvy,C., Malthete,J. and Silberzan,P. (2003) Functionalizing surfaces with nickel ions for the grafting of proteins. *Langmuir*, **19**, 4138–4143.
35. Sigal,G.B., Bamdad,C., Barberis,A., Strominger,J. and Whitesides,G.M. (1996) A self-assembled monolayer for the binding and study histidine-taged proteins by surface plasmon resonance. *Anal. Chem*., **68**, 490–497.
36. Gotch,M., Hasebe,M., Ohira,T., Hasegawa,Y., Shinohara,Y., Sota,J., Nakao,H. and Tosu,M. (1997) Rapid method for detection of point mutations using mismatch binding protein (MutS) and an optical biosensor. *Genet. Anal*., **14**, 47–50.
37. Sauerbrey,G. (1959) The use of quartz oscillators for weighing thin layers and for microweighing. *Z. Physik*, **155**, 206–222.